Available online at www.sciencedirect.com
SCIENCE DIRECT®

NUCLEAR SCIENCE AND TECHNIQUES

Nuclear Science and Techniques, Vol.17, No.3 (2006) 177–184

Experimental research on heat transfer to liquid sodium and its incipient boiling wall superheat in an annulus

XIAO Ze-Jun[1,2,*] ZHANG Gui-Qin[2] SHAN Jian-Qiang[2] BAI Xue-Song[1] JIA Dou-Nan[2]

([1]National Key Laboratory of Bubble Physics & Natural Circulation, Nuclear Power Institute of China, Chengdu 610041, China;
[2]School of Energy and Power Engineering, Xi'an Jiaotong University, Xi'an 710049, China)

Abstract Liquid sodium is mainly used as a cooling fluid in the liquid metal fast breeder reactor (LMFBR), whose heat transfer, whether convective heat transfer or boiling heat transfer, is different from that of water. So it is important for both normal and accidental operations of LMFBR to perform experimental research on heat transfer to liquid sodium and its boiling heat transfer. This study deals with heat transfer with high temperature (300–700°C) and low *Pe* number (20~70) and heat transfer with low temperature (250~270°C) and high *Pe* number (125~860), and its incipient boiling wall superheat in an annulus. Research on heat transfer involves theoretical research and experiments on heat transfer to liquid sodium. It also focuses on the theoretical analysis and experimental research on its incipient boiling wall superheat at positive pressure in an annulus. Semiempirical correlations were obtained and they were well coincident with the experimental data.

Key words Liquid sodium; Heat transfer; Incipient boiling; Wall superheat; Annulus

CLC number TL331

1 Introduction

Metal sodium is a very important chemical product. Although investigation on the heat-transfer characteristics of liquid sodium started in the 1940s, it has made great progress within these 30 to 40 years. Nowadays, liquid sodium is mainly used as a cooling medium in the liquid metal fast breeder reactor (LMFBR), and also as a working fluid in the space power station. Liquid sodium is a low-viscosity fluid with wettability, whose fluid mechanics characteristics are the same as those of water. Its low *Pr* number makes its thermal conductivity two orders of magnitude higher than that of ordinary fluids, and it also makes liquid sodium heat transfer, whether convective heat transfer or boiling heat transfer, different from that of ordinary fluids.

As concerns the present research of liquid-sodium heat transfer, although a thorough research has been done on single-phase forced convective heat transfer in fully developed region of velocity and temperature fields [1], the experimental research on heat transfer of liquid sodium with low *Pe* number and high temperature is yet to be studied in detail. It was also shown [2] that the mechanism of sodium boiling heat transfer itself needs considerable modification, and data of sodium incipient boiling wall superheat are even more decentralized. Several contradictory results may be obtained, which is attributed to factors such as different experimental conditions. It should be pointed out that it is of both academic and engineering values to enrich and perfect experimental research in this field for both normal and accidental operations of LMFBR.

*Corresponding author. E-mail: xzj670711@vip.sina.com
Received date: 2005-09-13

2 Theoretical research

2.1 Research on heat transfer

2.1.1 Derivation of differential equations

On the basis of similar assumptions as shown in Ref. [3], Eq. (A), composed of the mass, momentum, and energy balance equations (1), (2), and (3), can be written as

$$\left.\begin{aligned}&\frac{\partial \bar{u}}{\partial x}+\frac{\bar{\upsilon}}{r}+\frac{\partial \bar{\upsilon}}{\partial r}=0 &(1)\\ &\bar{u}\frac{\partial \bar{u}}{\partial x}+\bar{\upsilon}\frac{\partial \bar{u}}{\partial r}=-\frac{\partial p}{\rho \partial x}+\frac{\partial}{r\partial r}\left[(\upsilon+\varepsilon_m)r\frac{\partial \bar{u}}{\partial r}\right] &(2)\\ &\bar{u}\frac{\partial \bar{t}}{\partial x}+\bar{\upsilon}\frac{\partial \bar{t}}{\partial r}=\frac{\partial}{r\partial r}\left[(a+\varepsilon_h)r\frac{\partial \bar{t}}{\partial r}\right] &(3)\end{aligned}\right\}\text{(A)}$$

where $\bar{u}$, $\bar{\upsilon}$, and $\bar{t}$ represent the time average values of the corresponding parameters and their boundary conditions are shown in Eq. (B):

$$\left.\begin{aligned}&\bar{u}\big|_{r=r_1}=\bar{\upsilon}\big|_{r=r_1}=\bar{u}\big|_{r=r_2}=\bar{\upsilon}\big|_{r=r_2}=0 &(4)\\ &\bar{u}\big|_{x=0}=\bar{u}_{\text{in}} &(5)\\ &\bar{t}\big|_{x=0}=\bar{t}_{\text{in}} &(6)\\ &-k\frac{\partial \bar{t}}{\partial r}\Big|_{r=r_1}=q &(7)\\ &-k\frac{\partial \bar{t}}{\partial r}\Big|_{r=r_2}=0 &(8)\end{aligned}\right\}\text{(B)}$$

Since the fluid properties were assumed to be constant, Eq. (2) in Eq. (A) is not influenced by the temperature distribution. By solving Eqs. (1) and (2) simultaneously, the velocity distribution can be obtained. Then shift the solution to Eq. (3) and the temperature distribution can be obtained.

2.1.2 Solution of velocity field

Assuming:

$U=\bar{u}/\bar{u}_{\text{in}}$, $V=\bar{\upsilon}/\bar{u}_{\text{in}}$,

$B=(d_2-d_1)/d_1$, $Z=(x/D_e)/Re$,

$D_e=d_2-d_1$, $b=D_e/2$,

$r^*=r_2/r_1$, $R=(r-r_1)/(r_2-r_1)$,

$\beta(r)=\beta(R)=1+\varepsilon_m(R)/\upsilon$,

and solving Eqs. (1), (2), (4), and (5), the dimensionless equations of velocity field can be written as:

$$\left.\begin{aligned}&\frac{1}{(1+BR)}\times\frac{\mathrm{d}}{\mathrm{d}R}\left[\beta(R)(1+BR)\frac{\mathrm{d}U_w(R)}{\mathrm{d}R}\right]=\frac{\partial P}{\partial Z} &(9)\\ &U_w(0)=U_w(1)=0 &(10)\end{aligned}\right\}\text{(C)}$$

From Eq. (9), the left expression (LE) is only related to R, and the right expression (RE) is only related to Z, thus LE = RE = constant. Considering the constant as C_w and solving Eq. (9), the velocity distribution in a fully developed region can be obtained as follows:

$$U_w(R)=(1+B/2)\times\frac{\displaystyle\int_0^R\frac{(1+BR')}{\beta(R')}R'-\frac{\displaystyle\int_0^1\frac{(1+BR)}{\beta(R)}\mathrm{d}R}{\displaystyle\int_0^1\frac{\mathrm{d}R}{(1+BR)\beta(R)}}\int_0^R\frac{\mathrm{d}R'}{(1+BR')\beta(R')}}{\displaystyle\int_0^1(1+BR)\int_0^R\frac{(1+BR')}{\beta(R')}\mathrm{d}R'\cdot\mathrm{d}R\frac{\displaystyle\int_0^1\frac{(1+BR)}{\beta(R)}\mathrm{d}R}{\displaystyle\int_0^1\frac{\mathrm{d}R}{(1+BR)\beta(R)}}\int_0^1(1+BR)\int_0^R\frac{\mathrm{d}R'}{(1+BR')\beta(R')}\mathrm{d}R} \quad (11)$$

2.1.3 Solution of temperature field

To obtain the dimensionless equations of temperature field, it is necessary to make

$\bar{R}=r/r_1$,

$\bar{x}=Z/Pr$,

$$\Phi(\bar{x},\bar{R})=\frac{\bar{t}(\bar{x},\bar{R})-\bar{t}(\bar{x},1)}{qr_1/k},$$

$$\beta'(R)=1+\varepsilon_h/a=1+Pr\psi(\varepsilon_m/\nu),$$

and solve Eqs. (3), (6), (7), and (8). Then,

$$\left.\begin{aligned}
&\bar{R}\beta'\left(\bar{R}\right)\frac{\partial\Phi}{\partial R}=\frac{1}{4B^2}\times\left[\int_1^{\bar{R}}U\frac{\partial\Phi}{\partial\bar{x}}\bar{R}'\cdot\mathrm{d}\bar{R}'-\frac{2\int_1^{\bar{R}}U\bar{R}'\cdot\mathrm{d}\bar{R}'}{B\left(B+2\right)}\int_1^{r^*}U\frac{\partial\Phi}{\partial\bar{x}}\bar{R}'\cdot\mathrm{d}\bar{R}'\right]+\\
&\frac{Pe}{2B}\times\left[\int_1^{\bar{R}}V\frac{\partial\Phi}{\partial\bar{R}'}\bar{R}'\cdot\mathrm{d}\bar{R}'-\frac{2\int_1^{R}UR'\cdot\mathrm{d}\bar{R}'}{B\left(B+2\right)}\right]\times\int_1^{r^*}V\frac{\partial\Phi}{\partial\bar{x}'}\bar{R}'\cdot\mathrm{d}\bar{R}'-\beta'\left(1\right)\times\left[1-\frac{2\int_1^{\bar{R}}U\bar{R}'\cdot\mathrm{d}\bar{R}'}{B\left(B+2\right)}\right] &&(12)\\
&\Phi\left(0,\bar{R}\right)=0 &&(13)\\
&Nu\left(\bar{x}\right)=-B^2\left(B+2\right)/\int_1^{r^*}U\Phi\left(\bar{R}\right)\mathrm{d}\bar{R} &&(14)
\end{aligned}\right\}(D)$$

For the developed region, $V=0,\partial\Phi/\partial\bar{x}=0$, and Eq. (14) may be modified as

$$Nu_{\omega}=-B^2\left(B+2\right)/\int_1^{r}U\Phi\left(\bar{R}\right)\mathrm{d}\bar{R} \qquad (15)$$

2.1.4 Theoretical results

From Eqs. (11) and (15), the velocity and temperature field distributions can be obtained by numerical integral method. The theoretical results can be expressed by

$$Nu_{\omega}=4.40+0.019Pe^{0.8} \qquad (16)$$

It must be pointed out that the formulas of parameters such as ε_m, ε_h, ψ, and so on, were finally selected on the basis of the previous optimization. In principle, it is appropriate to the whole turbulent heat transfer in an annulus with the developed velocity and temperature fields.

2.2 Research on incipient boiling wall superheat

Incipient boiling is relative to steady boiling. Mechanism of incipient boiling is much more complicated than that of steady boiling. When boiling of any liquid happens on a heating surface, its surface temperature T_w must be higher than its saturation temperature T_s, and the difference of (T_w-T_s) is referred to as wall superheat. Forced convective boiling in an annulus can be treated as a combination of forced convection and pool boiling. On the basis of analysis and study of single-phase forced convective heat transfer and pool boiling heat transfer, the mathematic model of forced convective incipient sodium boiling heat transfer is obtained with the help of the superposition principle.

2.2.1 Single-phase forced convective heat transfer

It was shown [4] that an appropriate turbulent heat transfer correlation of liquid metal flowing in an annular is as follows:

$$Nu=\alpha+\beta(\Psi Pe)^{\gamma} \qquad (17)$$

where $\alpha=4.82+0.697d_2/d_1$, $\beta=0.022$, $\gamma=0.758(d_2/d_1)^{0.053}$. In the experiment, $d_2/d_1=1.67$; therefore, Eq. (17) can be written as:

$$Nu=5.98+0.022(\Psi Pe)^{0.779} \qquad (18)$$

where $\Psi=1-1.82/[Pr(\varepsilon_m/\upsilon)^{1.4}]$, $(\varepsilon_m/\upsilon)=4.0+0.0029Re^{0.919}$. And then:

$$q_c=[5.98+0.022(\Psi Pe)^{0.779}]K(T_w-T_f)/D_e \qquad (19)$$

2.2.2 Pool boiling heat transfer

Presently, the theoretical model of sodium pool nuclear boiling is put forth on the basis of general boiling mechanism research. It has been shown [5] that the correlation is as follows:

$$h_n=mP_L^{0.27}q_n^{0.68} \qquad (20)$$

And then the following expression is obtained:

$$q_n=nP_L^{0.844}(T_w-T_s)^{3.125} \qquad (21)$$

2.2.3 Forced convective incipient boiling heat transfer

Although there are many factors which influence the incipient boiling superheat, such as heat flux, pressure, velocity, subcooling, detained inert gas concentration on wall, oxide impurity content in sodium, roughness of heating surface, physicochemical characteristics of fluid, wettability, and so on, the important factors are heat flux, pressure, and velocity. It has been shown that the total heat flux of forced convective boiling equals the convective heat flux plus pool boiling heat flux [6]. Incipient boiling heat transfer combines forced convective heat transfer and pool boiling heat transfer, and the correlation is as follows:

$$q=S_cq_c+F_nq_n \qquad (22)$$

From Eqs. (19) and (21),

$$q = S_c[5.98 + 0.022(\Psi Pe)^{0.779}]K(T_w - T_f)/D_e + F_n n P_L^{0.844}(T_w - T_s)^{3.125} \quad (23)$$

Considering the actual conditions in these experiments, Eq. (23) is simplified as follows:

$$q = M[5.98 + 0.022(\Psi Pe)^{0.779}] + NP_L^{0.844}(T_w - T_s)^{3.125} \quad (24)$$

It is well known that Ψ equals zero under low *Re* number. So the effect of velocity on wall superheat under low velocity is not considered in Eq. (24). However, the experiments show that the low velocity influences the incipient boiling superheat to a great extent. So Eq. (24) is modified as follows:

$$q = M[5.98 + 0.022(\Psi Pe)^{0.779}] + NP_L^{0.844}(T_w - T_s)^{3.125} Pe^C \quad (25)$$

3 Research on heat transfer

3.1 Heat transfer with high temperature and low *Pe* number

The experiments were carried out in the sodium heat transfer test facility of Xi'an Jiaotong University (Fig.1). The test section is composed of an outer duct of 10 mm inner diameter and an electrical heating element of 6 mm outer diameter with a heat flux of 1500 $kW \cdot m^{-2}$ (Fig.2). The heating element is installed at the center of the outer duct. There are six small grooves at an equal angle of 60°, where six thermocouples of 0.3 mm diameter are installed at an equal distance of 10 mm. To ensure the radial fixity of the heating element, two fixed hoops are installed at the inlet and outlet of the outer duct.

The main experimental parameters are: temperature, 300~700°C; *Pe* number, 20~70; *Re* number 4000~17500; and oxide impurities 20~50 $\mu g \cdot g^{-1}$. Before the start of a set of experiments, heat balance tests were carried out to verify the reliability of the measuring system. The heat balances were no less than 95%. On the basis of experimental data, the following conclusions can be drawn:

(1) 60 sets of experimental data have been obtained. Heat transfer correlation is as follows:

$$Nu = 4.55 + 0.027 Pe^{0.971} \quad (26)$$

(2) Relative errors of experimental data are less than ±10%, whose decentralization degree is less than ±12%.

3.2 Heat transfer with low temperature and high *Pe* number

The experiments were also carried out in the sodium heat transfer test facility of Xi'an Jiaotong University. The test section is similar in structure to that used for the study of heat transfer with high temperature and low *Pe* number. It is composed of outer duct of 19 mm inner diameter and electrical heating element of 12.3 mm outer diameter with a heat flux of 500 $kW \cdot m^{-2}$. The heating element is installed at the center of the outer duct.

The main experimental parameters are: temperature, 250~270°C; *Pe* number, 125~860; *Re* number, $0.20 \times 10^5 \sim 1.35 \times 10^5$; and oxide impurities, 20~50 $\mu g \cdot g^{-1}$. The heat balances were no less than 95%. On the basis of experimental data, the following conclusions can be drawn:

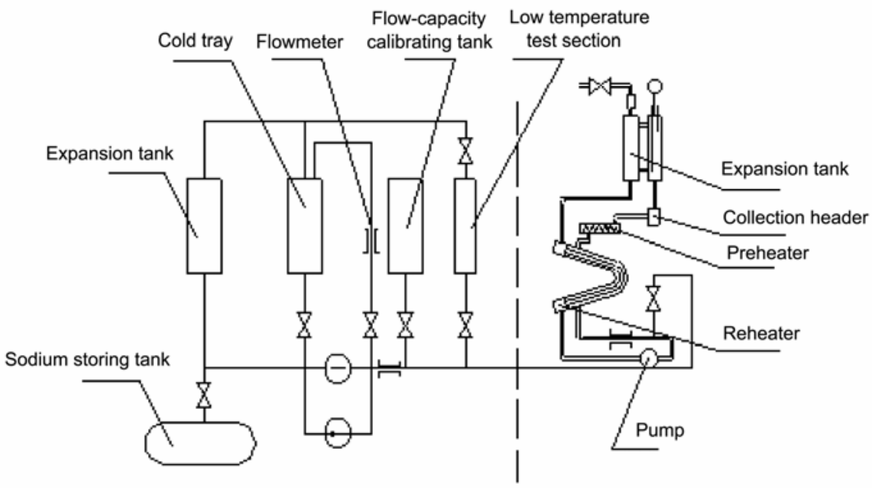

Fig.1 Schematic diagram of the sodium heat transfer test facility.

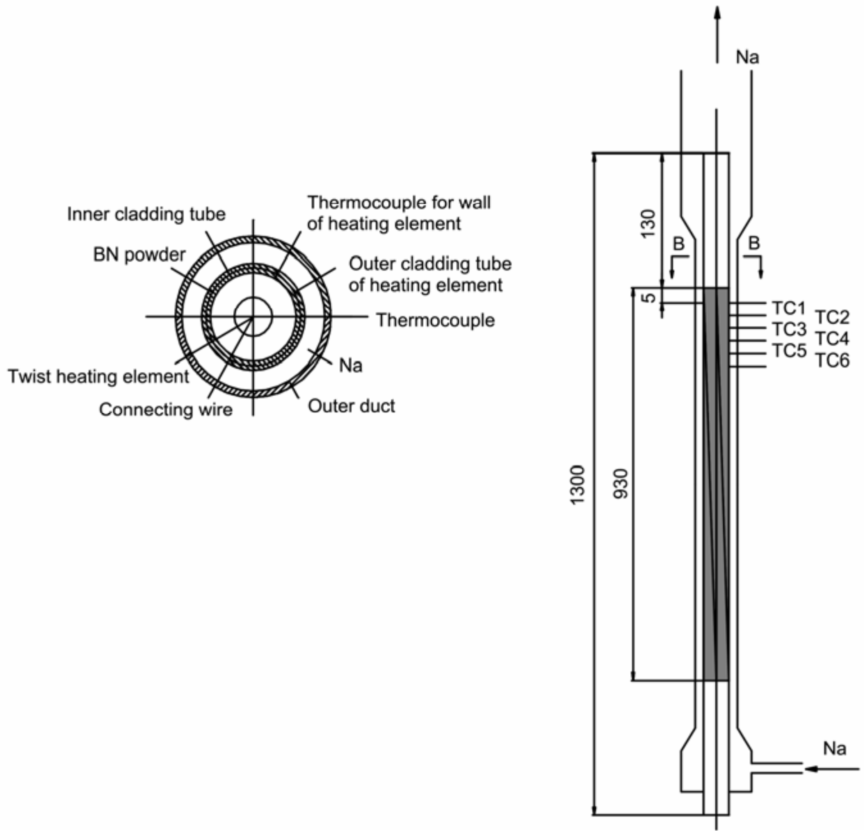

Fig.2 Schematic diagram of the test section. The left section shows an enlarged scale drawing of B-B section in the right drawing.

(1) 100 sets of experimental data have been obtained. The present results coincide with Eq. (16) very well.

(2) Relative errors of experimental data are less than ±14%, whose decentralization degree is less than ±7%.

3.3 Discussion

(1) Nowadays there are few articles in professional magazines that deal with heat transfer to high-temperature sodium with incipient and less developed turbulent flow. For further discussion and analysis, several data of similar conditions are selected for comparison (Fig. 3).

a) Eq. (18) is appropriate for the fully developed turbulent liquid metal flow; however, it does not fit the less developed turbulent flow because the value of ψ is negative when $Pe<250$. In these conditions, the heat transfer may be described by the constant term of molecular heat conduction expressed by curve 1 in Fig. 3. The present flow regime for liquid sodium with low *Pe* number basically belongs to the incipient and less developed turbulent flow.

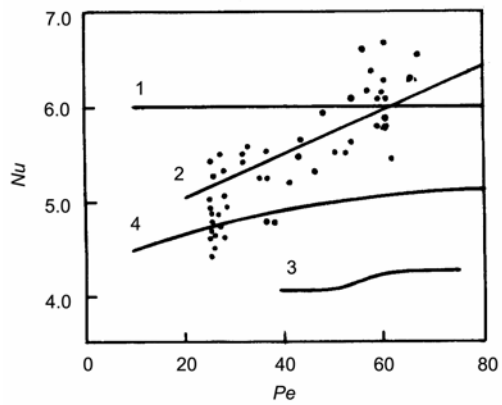

Fig.3 *Nu* vs. *Pe* for heat transfer with high temperature and low *Pe* number.

b) Eq. (26) (curve 2 in Fig.3) based on the experimental data describes the heat transfer to liquid sodium with high temperature and low *Pe* number in an annulus. It shows that neither turbulent eddy heat transfer nor molecular heat conduction can be ignored even in the region of incipient turbulent flow and less developed flow.

c) The heat transfer data of liquid sodium (with *Pe*, 40~100; temperature, 240~270°C; oxide impurity content, 100~300 $\mu g \cdot g^{-1}$) in an annulus are given in

Ref. [7]. The heat transfer curve 3 with *Pe* of 40~80 is shown in Fig. 3.

d) Curve 4 in Fig. 3 (Eq. (16)) is better than curve 3 although it is a little lower as compared with curve 2 in Fig. 3.

(2) Eq. (16) (curve 1 in Fig. 4) has been proved by the heat-transfer experiments with low temperature and high *Pe* number. For high *Pe* number heat transfer to liquid sodium in an annulus, there are a lot of experimental data which may be decentralized, but most of the investigators believe that Eqs. (17) and (18) are acceptable although they show a little larger *Nu* number in the high *Pe* number. As shown above, according to Eq. (16), the *Nu* number is only 8% (max.) lower than that in accordance with Eq. (18) as shown in Fig. 4 (curve 3).

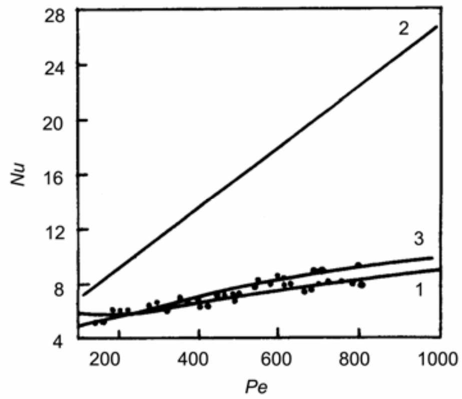

Fig.4 *Nu* vs. *Pe* for heat transfer with low temperature and high *Pe* number.

(3) Fig. 3 shows that the *Nu* number given by Eq. (26) and expressed by curve 2 is medium among all the curves shown in the figure. Ignoring the difference in experimental regimes among the curves in Fig. 3, even for the condition they represent, will also cause errors in different degrees because of the neglect of natural convection, axial heat transfer (which cannot be ignored for liquid metal laminar flow heat transfer), oxide impurity content, and so on, when they are derived or obtained. It is a typical example that the *Nu* number given by curve 3 in Fig. 3 is on the low side. The research shows that the inert gas on the heating wall may have a bad effect on heat transfer and especially on the velocity of laminar flow.

Eq. (26) is a sole correlation of heat transfer to liquid sodium with high temperature and low *Pe* number. However, it is not applicable to liquid sodium with low temperature and high *Pe* number as shown in Fig. 4 (curve 2).

4 Research on incipient boiling wall superheat

It has been shown that the incipient boiling wall superheat of liquid sodium is six times higher than the steady boiling wall superheat, and is about five times higher than that of water, which are attributed to the following facts: (1) within the range of general pressure and temperature, the pressure gradient $\partial P/\partial T$ of liquid sodium saturation pressure curve is comparatively small; (2) besides the active chemical feature of liquid sodium that has considerable effect on its self-cleaning for the heating surface, the high wettability makes surface activation nucleating difficult; (3) the detained inert gas on wall cavities helps bubbles nucleate, and the high temperature of sodium is apt for the removal of gas. Due to the complexity of the mechanism of liquid sodium incipient boiling, up to now the researches on this subject are just in the initial stage.

4.1 Experimental research

The experiments were carried out in the sodium heat transfer test facility of Xi’an Jiaotong University [8]. The test section in structure is the same as that used in the research on heat transfer with high temperature and low *Pe* number. The inlet flow rate is measured by a permanent magnetic flowmeter. The inlet and outlet pressures of the test section are measured by pressure sensors. A function recorder is used to follow up and record flow rate, pressure, and temperature fluctuating signals under boiling condition.

The main experimental parameters are: heat flux, 80~130 $\mathrm{kW{\cdot}m^{-2}}$; system pressure $1.09\times10^5\sim1.26\times10^5$ Pa; incipient boiling velocity, $0.02\sim0.14\ \mathrm{m{\cdot}s^{-1}}$; wall superheat, 8~35°C; oxide impurities 20~50 $\mathrm{\mu g{\cdot}g^{-1}}$. The heat balances were no less than 95%. On the basis of experimental data, the following conclusions can be drawn:

(1) 30 sets of experimental data have been obtained. Incipient boiling wall superheat is as follows:

$$T_W-T_S=0.921[q-8348.1-31(\Psi Pe)^{0.779}]^{0.32}P_L^{-0.27}Pe^{-0.544} \quad (27)$$

(2) Decentralization degree of experimental data are within ±19%.

4.2 Liquid sodium boiling fluctuation curve

When subcooling fluid flows upward in a vertical annulus, according to the heat transfer characteristics of forced convective boiling, several regions can be specified as follows: (1) single-phase region; (2) transition region from single phase to subcooling boiling; (3) unsteady subcooling boiling region; (4) steady subcooling boiling region; (5) saturation boiling region; and (6) liquid-deficient region. For unsteady subcooling boiling region, the subcooling of bulk fluid is large and the bubbles that are formed on the wall do not get the required supply of energy to grow, and hence cannot overcome the wall adhesive force to separate from the wall. The flow rate may be reduced because of the increased frictional pressure drop caused by numerous bubbles. For steady subcooling boiling region, the subcooling of bulk fluid decreases to approach zero, the bubbles on the wall get the required supply of energy to grow and to separate from the wall, and then enter the bulk fluid region. When the wall temperature, liquid temperature, and the flow rate decrease in various degrees, fluctuation occurs. The steady incipient boiling just starts. In other words, the place of the maximum wall temperature of the heating elements means the starting point of incipient boiling before the parameters fluctuate. Generally speaking, with the help of temperature, pressure, and flow fluctuation signals, the occurrence of incipient boiling can be determined effectively. The key sign of saturation boiling is that the bulk temperature reaches the saturation temperature. Figs. 5 and 6 show the fluctuation curves of subcooling boiling and saturation boiling, respectively. When subcooling boiling occurs under low velocity, outlet pressure of the test section fluctuates slightly, in connection with the process of bubble formation, growth, and breaking on the top part of the heating elements. When saturation boiling occurs under low velocity, the inlet pressure fluctuates more than the outlet pressure, which is associated with the pressure compensation of the expansion tank. For both regimes, the velocity fluctuations are very obvious, and frequencies and amplitudes of the fluctuation are quite different.

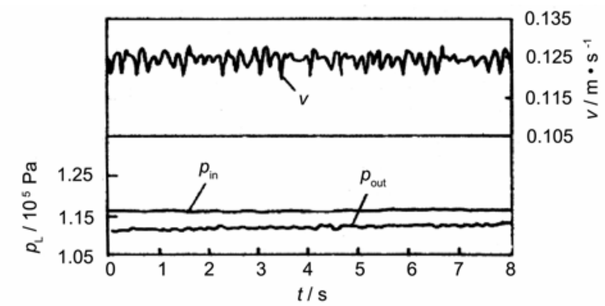

Fig. 5 Fluctuating curves of subcooling boiling.

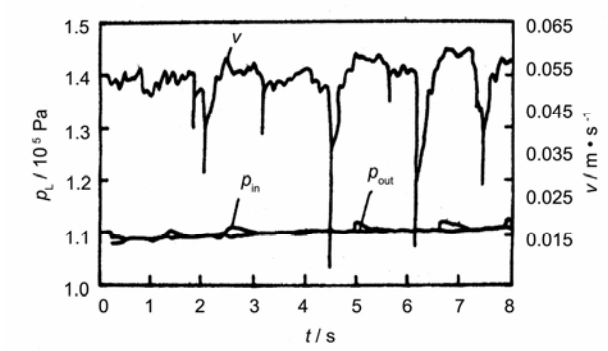

Fig. 6 Fluctuating curves of saturated boiling.

5 Conclusions

On the basis of experimental data and theoretical research on heat transfer to liquid sodium and its incipient boiling wall superheat in an annulus, the following conclusions can be drawn:

(1) The formula of heat transfer with high temperature and low *Pe* number is obtained. Relative errors of experimental data are less than ±10%, with a decentralization degree of less than ±12%.

(2) The present results on heat transfer with low temperature and high *Pe* number coincide with the theoretical research. Relative errors of experimental data are less than ±14%, with a decentralization degree of less than ±7%.

(3) Incipient boiling wall superheat is obtained. The decentralization degree of experimental data is within ±19%.

Nomenclature

a Molecular thermal diffusivity ($m^2 \cdot s^{-1}$)

B Dimensionless width of annulus

b Width of annulus channel (m)

De Hydraulic equivalent diameter (m)

d_1, d_2 Inner and outer diameters (m)

F_n, S_c Correction factor

h_n Pool boiling heat transfer coefficient ($W \cdot m^{-2} \cdot °C^{-1}$)

K Thermal conductivity ($W \cdot m^{-3} \cdot °C^{-1}$)

M, N, C Parameters defined by experiment

m, n Coefficients

Nu, Nu_ω Nusselt number

P_L Pressure (Pa)

Pe Peclet number

Pr Prandtl number

q Heating flux ($W \cdot cm^{-2}$)

q_c Single-phase forced convection heat flux ($W \cdot cm^{-2}$)

q_n Pool boiling heat flux ($W \cdot cm^{-2}$)

R Dimensionless width variable of annulus

$\overline{R}$ Dimensionless radius

r Annular radius ($r_1 \leq r \leq r_2$, m)

r_1, r_2 Inner and outer radii of annulus (m)

r^* Radius ratio (r_2/r_1)

Re Reynolds number

t_{in}, t_{out} Inlet and outlet temperatures (°C)

T_f Temperature of liquid sodium (°C)

T_s Saturation temperature of liquid sodium (°C)

T_w Wall temperature of heating element (°C)

$\overline{t}$ Liquid temperature (°C)

U Dimensionless axial velocity

$\overline{u}$ Axial velocity ($m \cdot s^{-1}$)

$\overline{u}_{in}$ Inlet velocity ($m \cdot s^{-1}$)

V Dimensionless radial velocity

$\overline{\upsilon}$ Radial velocity ($m \cdot s^{-1}$)

x Axial coordinate (m)

$\overline{x}$ Dimensionless axial coordinate relative to Pe

y, z Coordinate (m)

Z Dimensionless axial coordinate relative to Re

Greek symbols

β Ratio of overall eddy diffusivity for momentum to kinematic viscosity

δ Temperature modification factor due to grooving wall of the heating element (°C)

ε_h Eddy diffusivity for heat transfer ($m^2 \cdot s^{-1}$)

ε_m Eddy diffusivity for momentum transfer ($m^2 \cdot s^{-1}$)

ν Kinematic viscosity ($m^2 \cdot s^{-1}$)

ρ Density of sodium ($kg \cdot m^{-3}$)

τ_1, τ_2 Shear stress of inner and outer walls of channel ($N \cdot m^{-2}$)

ϕ Dimensionless temperature

ψ Ratio of eddy diffusivity of heat to eddy diffusivity of momentum

References

1 Dwyer O E. Int J Heat Mass Transfer, 1969, **12**: 1403-1419.

2 Kottowski H M, Savatteri C. Int J of Heat and Mass Trans, 1977, **11**, 1281-1300.

3 Zhang Guiqin, Zhao Shurong, Jia Dounan. Heat and Technology, 1991, **9**: 135-145.

4 Dwyer O E, Tu P S. Nucl Sci Eng, 1964, **21**: 90-105.

5 Holtz R E, Singer R M, On the initiation of pool boiling in sodium, Proceedings of 10th National Heat Transfer Conference, Philadelphia, 1968, ASME:11-14.

6 Butterworth D, Hewitt G F. Two-phase flow and heat transfer, Oxford Univ. Press, 1977: 84-91.

7 Romanowa L A. Liquid metal, Russian National Atomic Energy Press, 1963, 153-156 (in Russian).

8 Xiao Zejun, Jia Dounan, Zhang Guiqin. The investigation of incipient sodium boiling wall superheat in a concentric annulus, The 3rd JSME/ASME joint international conference on nuclear engineering. 1, Kyoto, Japan, 1995, 53-58.